Articles

Interaction between the Antiapoptotic Protein Nr-13 and Cytochrome *c*. Antagonistic Effect of the BH3 Domain of Bax†

Mahnaz Moradi-Améli,*,‡ Thierry Lorca,§ Damien Ficheux,‡ Attilio di Pietro,‡ and Germain Gillet‡

Institut de Biologie et Chimie des Protéines, CNRS-UCBL UMR 5086, 7, Passage du Vercors, 69367 Lyon cedex 7, France, and Centre de Recherches de Biochimie Macromoléculaire, CNRS-UPR 1086, 1919 route de Mende, 34293 Montpellier cedex 5, France

Received May 21, 2001; Revised Manuscript Received April 8, 2002

ABSTRACT: Mitochondria act as a focal point for upstream apoptosis signals by releasing cytochrome *c* into the cytosol, leading to the activation of caspases and subsequent cell death. Members of the Bcl-2 protein family regulate this phenomenon by heterodimerization via the BH3 domain of proapoptotic members opposing their pro- and antiapoptotic functions. The mechanism of cytochrome *c* release from mitochondria and of its regulation remains controversial. In vitro binding studies of purified and biologically active proteins should help in understanding the molecular mechanism of interactions and protein functions. In this work, the Bcl-2-related antiapoptotic chicken protein Nr-13 was overexpressed as a highly soluble recombinant protein which showed correct folding as judged by circular dichroism and fluorescence spectroscopy. Purified Nr-13 inhibits caspase-3 activation in a *Xenopus* egg-derived cell-free system, and neutralizes the proapoptotic activity of a synthetic peptide containing the BH3 domain of Bax. The latter effect correlates with the high-affinity binding of the BH3 peptide to Nr-13 as monitored by the intrinsic tryptophan fluorescence. On the basis of the structural similarity with Bcl-x_L, putative residues involved in this interaction were identified. Nr-13 exhibits a high-affinity interaction with cytochrome *c* which is prevented by preincubation with the BH3-Bax peptide. These findings are discussed with respect to a model for the regulation of apoptosis in which a direct interaction between the antiapoptotic protein and cytochrome *c* may prevent the apoptosis.

Proteins of the Bcl-2 family are central regulators of apoptosis, and several of its members are evolutionarily conserved in both vertebrates and invertebrates (*1*, *2*). Bcl-2 proteins play important roles in embryogenesis, tissue remodeling, and the immune response by acting as either inhibitors or promoters of apoptosis (*2*, *3*). Aberrant expression of Bcl-2 proteins has been correlated to many diseases such as autoimmunity, neurodegenerative disorders, and cancer (*4*). These proteins control cell survival through their effects on events such as mitochondrial release of proteins such as cytochrome *c* or Smac/Diablo. The latter proteins are involved in the activation of caspases, the apoptosis-associated cystein proteases. This activation initiates an execution and degradation phase upon which downstream caspases become activated and catalyze the morphological and biochemical changes leading to apoptosis (*2*, *5*, *6*).

Bcl-2 proteins share up to four regions of sequence similarity known as Bcl-2 homology domains BH1, BH2, BH3, and BH4. Some Bcl-2 proteins contain a stretch of hydrophobic residues at their C-terminus which is predicted to be a transmembrane domain (*2*). Many proteins of the Bcl-2 family can interact with each other to form homo- or heterodimers. These interactions play important roles in the opposing effects of proapoptotic (Bad, Bax, Bak, Bid, Bim, and Bcl-x_s) and antiapoptotic (Bcl-2, Bcl-x_L, Bcl-w, and Nr-13) Bcl-2 proteins (*2*, *5*). The three-dimensional structures of Bcl-x_L, Bid, and Bax have been determined, revealing a common protein fold consisting of seven or eight α-helices joined by flexible loops of variable length (*7*−*10*). The BH1, BH2, and BH3 domains are in spatial proximity and form an elongated hydrophobic cleft (*7*). The antagonistic effects of the proapoptotic members depend on the binding, via their BH3 domains, to the hydrophobic cleft of antiapoptotic proteins (*10*). A hairpin pair of central α-helices shares structural similarity with pore-forming domains of bacterial toxins, and they may participate in membrane insertion of Bcl-2 proteins (*7*). Consistent with this idea, recombinant proteins have been shown to form ion channels when reconstituted into synthetic lipid membranes (*11*−*13*).

† This work was supported by La Ligue Nationale Contre le Cancer-Comité de la Drôme, the Association pour la Recherche sur le Cancer, the Centre National de la Recherche Scientifique, and the Université Claude Bernard Lyon 1.

* To whom correspondence should be addressed: IBCP, 7 passage du Vercors, 69367 Lyon cedex 7, France. Telephone: (33) 472 72 26 11. Fax: (33) 472 72 26 04. E-mail: m.moradi@ibcp.fr.

‡ CNRS-UCBL UMR 5086.

§ CNRS-UPR 1086.

10.1021/bi0110286 CCC: $22.00
Published on Web 06/14/2002

Cytochrome *c* is the most prominent member within the mixture of proapoptotic proteins sequestered in mitochondria. Following translocation of proapoptotic proteins to the outer membrane, mitochondrial release of cytochrome *c* is a critical step in apoptotic signal transduction since besides Apaf-1 it is one of the components required for activation of caspase-9 and formation of the apoptosome complex in the cytosol (*6*). This process has been studied extensively, leading to the development of several models for cytochrome *c* release, including an increase in the mitochondrial outer membrane permeability (*14*), and involvement of specific channels, called permeability transition (*15*). Although the antiapoptotic members of the Bcl-2 family can antagonize the effect of apoptotic proteins through heterodimerization, several other mechanisms of regulation have been proposed for the antiapoptotic members. These include prevention of the loss of mitochondrial membrane potential by either stimulation of proton efflux (*16*) or maintenance of ATP−ADP exchange (*17*). Overexpression of Bcl-2 inhibited apoptosis and blocked the release of cytochrome *c* (*18*, *19*). A voltage-dependent anion channel, which is part of the permeability transition pore, plays a critical role in the release of cytochrome *c* (*20*). Bax or Bak induces an efflux of cytochrome *c* by opening this channel, whereas Bcl-x_L closes it by binding to it. The mechanism by which cytochrome *c* is retained in the intermembrane space, however, remains obscure. Understanding this mechanism is therefore an important step toward the elucidation of the pathway of apoptosis regulation.

Although various proteins of the Bcl-2 family exhibit structural and functional similarities, they harbor nonredundant roles in regulating cell survival and death in specific tissues. Thus, it is important to identify the molecular mechanism of action of each member of the Bcl-2 family. This work has focused on Nr-13, an avian Bcl-2-related protein, which was originally identified as an antiapoptotic protein involved in tumor formation upon infection by Rous sarcoma virus (*21*, *22*). Nr-13 plays a major role in the regulation of cell death in B-cells during the development of the immune system in the chicken bursa (*23*). To elucidate the molecular mechanism of its antiapoptotic function, we used a recombinant Nr-13 protein purified to homogeneity in its biologically active form. Here we show that the recombinant protein acts as an inhibitor of apoptosis in a cell-free system and prevents the opposing effect of a synthetic peptide derived from the proapoptotic Bax protein containing the BH3 domain. This prevention correlates with the high-affinity interaction between Nr-13 and the BH3 peptide. We also found that Nr-13 exhibits a high affinity for cytochrome *c* which competes with its BH3-dependent interaction. This suggests that the release of cytochrome *c* from mitochondria may be prevented by its direct interaction with antiapoptotic Nr-13 and that Bax inhibits this interaction.

EXPERIMENTAL PROCEDURES

Cloning and Generation of the Expression Plasmid. A cDNA encoding Nr-13 lacking the C-terminal hydrophobic region (residues 1−157) was amplified by standard PCR using a full-length chick cDNA as a template. At the 3′-end, the primer sequence 5′-CTGCAGCTGCAGATTGCTTAAGGTACTGTT-3′ introduced a *Pst*I site, and at the 5′-end, the primer sequence 5′-CAGATGTAGACATATGCCGGGCTCTCTGAAG-3′ introduced a *Nde*I site. The PCR-generated DNA fragment was cloned into the *Nde*I and *Pst*I sites of the ampicillin-resistant vector pT7-7 (a vector based on the T7 polymerase expression system) encoding six His codons followed by a stop codon downstream of the *Pst*I site. The plasmid was transformed into *Escherichia coli* strain DH5α, and ampicillin-resistant colonies were isolated. Resistant colonies were grown to allow large-scale production and purification of the plasmid. Its proper construction was confirmed by DNA sequencing.

Overexpression and Purification of Nr-13. The plasmid was transformed into *E. coli* strain C41(DE3) (*24*). A freshly transformed colony was inoculated into 500 mL of 2× YT medium containing ampicillin (20 μg/mL) and grown at 37 °C to an OD_{600} of 0.6−0.8 before induction with 0.7 mM isopropyl β-D-thiogalactopyranoside. After overnight incubation at 37 °C, cells were harvested by centrifugation. The pellet was suspended and incubated for 30 min at 4 °C in 10 mL of lysis buffer [20 mM Tris-HCl (pH 8.0), 20% glycerol, 500 mM NaCl, 0.1% Triton X-100, 5 mM PMSF,[1] 5 mM dithiothreitol (DTT), 10 mM imidazole, 1 mg/mL lysozyme, and 250 units/mL Benzonase (Merck)]. Fractions (1 mL) were disrupted by sonication for 5 × 7 s. After centrifugation at 12000*g* for 20 min, the soluble fraction was applied onto an 0.5 cm × 2 cm Ni−NTA−agarose column (Qiagen) equilibrated in lysis buffer without lysozyme and Benzonase. The column was washed with 20 mM Tris-HCl (pH 8.0), 20% glycerol, 100 mM KCl, 5 mM DTT, 0.5 mM PMSF, and 20 mM imidazole, and Nr-13 was eluted with the same buffer containing 100 mM imidazole. Fractions containing Nr-13 as judged by SDS−PAGE were pooled and concentrated on Ultrafree Biomax membranes (Millipore) with a cutoff of 5 kDa.

The buffer of the concentrated samples was exchanged by gel filtration (PD10, Bio-Rad) with buffer A [20 mM Tris (pH 8.0), 50 mM NaCl, 10 mM EDTA, 10 mM DTT, and 0.5% 2-propanol], and samples were applied to two 1 mL Q-Sepharose columns (Hi-Trap Q, Amersham Pharmacia Biotech) in series. After elution, Nr-13-rich fractions were pooled, concentrated, equilibrated in buffer B [20 mM Tris (pH 8.0), 10 mM EDTA, 10 mM DTT, and 5% 2-propanol], and applied to another 1 mL Hi-Trap Q column. After extensive washing, a linear gradient of 0 to 300 mM NaCl in buffer B was applied. Fractions containing Nr-13 were pooled, concentrated to 1−6 mg/mL on an Ultrafree Biomax membrane, and stored at −20 °C until they were used. Protein concentrations were determined by the method of Bradford (*25*).

Analysis of Purified Nr-13. N-Terminal sequencing of Nr-13 was carried out on an Applied Biosystems 473A sequencer as described previously (*26*). Mass spectra were acquired using an electrospray API 16S Sciex (Perkin-Elmer) instrument. Drawing was made in 50% methanol containing 0.1% formic acid at a flow rate of 10 μL/h on a micro-ion-

[1] Abbreviations: AMC, amino-4-methylcoumarine; BH3-Bax, 29-mer synthetic peptide containing the BH3 domain of Bax; CD, circular dichroism; DTT, dithiothreitol; MMR, modified Ringer's solution; ELISA, enzyme-linked immunosorbent assay; NATA, *N*-acetyltryptophanamide; NTA, nitrilotriacetic acid; PARP, poly(ADP-ribose) polymerase; PMSF, phenylmethanesulfonyl fluoride; PT, permeability transition; SDS−PAGE, SDS−polyacrylamide gel electrophoresis; TBS, Tris-buffered saline; VDAC, voltage-dependent anion channel.

spray source as described by the manufacturer. Nr-13 was loaded onto a Vydac C18 5 μm (4.6 mm × 250 mm) reverse-phase column equilibrated in 35% acetonitrile and 0.1% trifluoroacetic acid. The column was developed for 20 min with a 35 to 70% acetonitrile gradient in 0.1% trifluoroacetic acid, and the eluted protein was passed directly into the mass spectrometer. Analytical size-exclusion chromatography was performed using the Superose 12 column (Amersham Pharmacia Biotech) on a Waters 625 LC HPLC system. The running buffer was 5 mM MOPS (pH 7.5), 200 mM NaCl, and 2 mM DTT. After equilibration, 90 μL of Nr-13 at a concentration of 0.45 mg/mL in the above buffer was loaded onto the column. The column (24 mL) was run at a flow rate of 0.4 mL/min for 60 min. Detection of the eluted protein was carried out at 280 nm. The column was calibrated with molecular mass standard proteins. For circular dichroism (CD) measurements, 40 μM Nr-13 samples in 20 mM Tris (pH 8), 10 mM EDTA, 5% 2-propanol, and 0.5 mM DTT were used. CD spectra were recorded on a Jobin Yvon CD6 spectropolarimeter equipped with a temperature controller using a 2 mm path length quartz cell. The α-helical content was estimated from the molar ellipticities observed at 222 nm (*27*).

Peptide Synthesis and Cross-Linking. A synthetic peptide, BH3-Bax, with the sequence VPQDASTKKLSECLKRIGDELDSNMELQR corresponding to residues 50−78 of human proapoptotic Bax containing the BH3 domain (underlined) was synthesized using *N*-(9-fluorenyl)methoxycarbonyl chemistry and the solid-phase method (*28*). The peptide was purified by reverse-phase chromatography on a C18 column (10 mm × 250 mm) developed with a 0 to 53% acetonitrile/0.1% trifluoroacetic acid gradient for 90 min. The correct molecular mass was confirmed by mass spectroscopy (see above).

For cross-linking experiments, Nr-13 (15 μM) was incubated for 10 min in the absence or presence of stoichiometric amounts of BH3-Bax in 20 mM MOPS (pH 7.5), 0.1 M NaCl, and 2 mM DTT in a final volume of 26 μL, before the addition of glutaraldehyde to a final concentration of 0.06%. The reaction was allowed to continue for 20 min and stopped by the addition of electrophoresis sample buffer and heating. Reaction products were analyzed by SDS−PAGE.

Immunoassay. The level of binding of Nr-13 was determined by an ELISA using microtitration plates (Greiner) coated overnight with 2.5 μg of cytochrome *c* (horse heart, Sigma C7150) per well in 10 mM sodium phosphate (pH 7.0). Nonspecific sites were blocked by a 1 h incubation at room temperature with TBS [10 mM Tris (pH 7.2) and 0.15 M NaCl] containing 1.5% bovine serum albumin. The plates were incubated for 1 h with 100 μL of various amounts of Nr-13 in TBS containing 1 mM DTT, 0.5% bovine serum albumin, and 0.05% Tween 20. After being washed with TBS containing 0.1% Tween 20, the plates were incubated for 1 h with mouse anti-His antibody (Roche) followed by washing and incubation (1 h) with peroxidase-conjugated anti-mouse antibody (Dako). After four washes, the binding of Nr-13 was detected by addition of peroxidase substrate [0.9 mM 2,2′-azinobis(3-ethylbenzo-6-thiazolinsulfonic acid), 2.9 mM H_2O_2, 0.1 M sodium phosphate, and 80 mM sodium citrate (pH 4.0)]. Absorption was measured at 405 nm with an ELISA plate reader. When indicated, the binding of Nr-13 to microtitration plates coated with lysozyme (2.5 μg/well), as a control, was assessed under the same conditions.

Fluorescence Spectroscopy. Experiments were performed on a SLM-Aminco 8000C spectrofluorimeter using bandwidths of 2 and 4 nm for excitation and emission, respectively. Measurements were corrected for the wavelength dependence on the excitation light intensity using rhodamine B in the reference channel. Fluorescence measurements were performed at 25 °C after dilution of Nr-13 (final concentration of 0.4 μM) in 1.2 mL of 20 mM Tris (pH 8.0), 0.1 M NaCl, 10% glycerol, and 1 mM DTT. The tryptophan intrinsic fluorescence of Nr-13 was measured by scanning emission in the range of 310−460 nm upon excitation at 295 nm. Binding of either cytochrome *c*, its heme (microperoxidase from equine heart, Sigma), or BH3-Bax was monitored by the quenching of emission fluorescence of Nr-13 produced by addition of increasing concentrations of ligand; spectra were recorded 10 min after addition of each ligand. In parallel assays, 0.4 μM *N*-acetyltryptophanamide (NATA) was used instead of Nr-13 at the same ligand concentrations. Each spectrum (Nr-13 or NATA) was first corrected by subtraction of the buffer containing an identical concentration of ligand. Nr-13 spectra were then corrected for the inner-filter effect of the ligand, taking into account the extent of the NATA fluorescence decrease in the presence of a given ligand concentration. We verified that cytochrome *c*, which contains a single tryptophan that is completely quenched by energy transfer to the heme, does not exhibit any fluorescence by itself. Curve fitting of ligand binding related to the fluorescence decrease of Nr-13 was performed using GraFit (Erithacus software). The GraFit program takes into account the bound ligand to calculate free ligand concentrations and to determine the apparent K_D values, as described in detail elsewhere (*29*).

Caspase Inhibition Assay in Xenopus Egg Extracts. *Xenopus* extracts were prepared by injection of 80 units of pregnant mare serum gonadotropin (Intervet) into mature female frogs to induce oocyte maturation followed 28 days later by injection of 600 units of human chorionic gonadotropin. One day after the last injection, eggs were harvested, and the apoptotic extracts were prepared as follows. Jelly coats were removed by incubation with 2% cysteine (pH 7.8). Eggs were activated with 2 mg/mL calcium ionophore (Sigma) in 0.5× modified Ringer's solution [MMR, 2.5 mM Hepes (pH 7.8), 50 mM NaCl, 1 mM KCl, 0.5 mM $MgSO_4$, 0.05 mM EDTA, and 1 mM $CaCl_2$]. They were washed three times with 0.25× MMR and four times with 10 mM Hepes (pH 7.7), 50 mM sucrose, 100 mM KCl, 1 mM $MgCl_2$, and 0.1 mM $CaCl_2$. Ten minutes after activation, eggs were lysed by centrifugation at 15000*g* for 20 min. The supernatant was supplemented with 2 mM ATP, 10 mM phosphocreatine, 25 μg/mL creatine phosphokinase, 7 mM $MgCl_2$, 0.2 mM leupeptine, and 10 μg/mL cytochalasin B. Extracts were spun at 100000*g* for 1 h, and the cytoplasmic layer containing the cytosolic as well as light and heavy membrane fractions (*30*) was collected and stored in aliquots at −80 °C.

The caspase inhibition assay was originally designed by Cosulich et al. (*31*) to mimic the cleavage of poly(ADP-ribose) polymerase by caspase 3 in the *Xenopus* egg extracts. Caspase-3 activity was measured by assaying the cleavage of a fluorogenic peptide (Ac-DEVD-AMC) based on the known cleavage-site sequence of poly(ADP-ribose) poly-

merase (DEVD↓G) (*32*). *Xenopus* extracts were incubated in the presence of either Nr-13 (final concentration of 20 μM), BH3-Bax (20 μM) and cytochrome *c* (2.5 μM), or the buffer in which Nr-13 was stored (control experiment). At different times, 10 μL samples were removed and incubated for 10.0 min at 25 °C with 50 μM Ac-DEVD-AMC (Calbiochem) in 50 mM Hepes (pH 7.5), 100 mM NaCl, 10 mM DTT, 1 mM EDTA, and 10% glycerol. After incubation, samples were diluted to 2 mL with PBS. Cleavage of Ac-DEVD-AMC was monitored with a fluorimeter using excitation and emission wavelengths of 380 and 460 nm, respectively. Because of the high protein content of the *Xenopus* egg extract, Nr-13 was used in the micromolar range in these assays.

RESULTS

Overexpression and Purification of Chick Nr-13. Expression of chick Nr-13 in the standard *E. coli* strain BL21DE3 was unsuccessful since the toxicity of the expression plasmid prevented transformation of *E. coli* host cells. To overexpress Nr-13 without cytotoxic effects, we successfully used the C41(DE3) strain (*24*) that grew to a high saturation cell density. Nr-13 devoid of the hydrophobic C-terminal region was expressed as a soluble protein. Due to the cloning strategy, the recombinant protein contained two extra amino acids (LQ) followed by a hexahistidine tag at its C-terminus. However, the protein band hardly could be detected on SDS−PAGE (Figure 1A, lane 2), and detection was only possible by Western blotting (data not shown). Subsequently, Nr-13 was purified from the soluble fraction by affinity chromatography on a Ni−NTA−agarose column eluted with 100 mM imidazole. At this stage, the protein could be visualized on SDS−PAGE as a band migrating with an apparent molecular mass of 18.5 kDa (Figure 1A, lane 3). Highly charged impurities were first bound to an ion exchange column run in 50 mM NaCl upon which Nr-13 appeared in the flow-through (Figure 1A, lane 4). In the absence of NaCl, Nr-13 was bound onto a further anion exchange column from which it was eluted with a salt gradient at ~60 mM NaCl. To prevent precipitation due to the low-salt conditions, 5% 2-propanol was added to the elution buffer. This step removed further contaminating proteins and resulted in rather pure Nr-13 (Figure 1A, lane 5). Analysis by reverse-phase chromatography showed a single homogeneous peak eluting at 17 min (60% acetonitrile) (Figure 1B). Approximately 0.5 mg of Nr-13 could be obtained from 1 L of culture medium.

Protein Characterization. Sequence comparison between Nr-13 and Bcl-x_L shows the presence of significant similarities within the BH domains (Figure 2A). The hydrophobic character of critical residues of Bcl-x_L involved in the interaction with the proapoptotic BH3 domain (*7*, *33*) is conserved in the Nr-13 sequence. In Bcl-x_L, these residues include F^{97} from BH3, V^{126}, L^{130}, and F^{146} from BH1, and F^{105}; in Nr-13, these residues correspond to L^{42} from BH3, V^{71}, L^{75}, and F^{92} from BH1, and F^{50}. The location of these residues within the three-dimensional structure of Bcl-x_L is shown either alone (Figure 2B; *7*) or in complex with BH3-Bax (Figure 2C; *10*).

N-Terminal sequencing of recombinant Nr-13 showed that the sequence start is PGSLKE (Figure 2A), which is identical with the cDNA-derived sequence of chick Nr-13 devoid of its first methionine residue. When the C-terminal replacement LQHHHHHH and the removal of the initiating methionine are taken into account, the recombinant Nr-13 protein consists of 164 amino acids corresponding to a calculated molecular mass of 17 768 Da. The same mass was determined by mass spectrometry (Figure 3). Analytical size-exclusion chromatography showed that the protein is present in two forms with apparent molecular masses of 70 and 18 kDa (Figure 1C), representing a 1/5 ratio as determined by integration of the chromatogram. The latter form corresponds to monomeric Nr-13, while the former probably represents

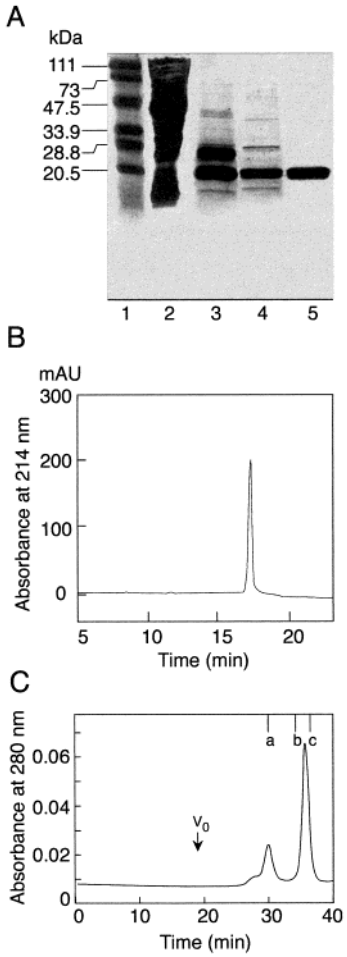

FIGURE 1: Purification and analysis of recombinant Nr-13. (A) The bacterial pellet obtained from a 500 mL culture of *E. coli* cells overexpressing the cDNA encoding Nr-13 was submitted to different purification steps (see Experimental Procedures), and samples from each step were analyzed by SDS−PAGE: lane 1, molecular mass markers; lane 2, total bacteria soluble proteins from the supernatant; lane 3, protein eluted by 100 mM imidazole from a Ni−NTA−agarose affinity column; lane 4, pool from the first Q-Sepharose high-performance column; and lane 5, purified protein eluted from the second Q-Sepharose high-performance column at 0.06 M NaCl. (B) Analytical reverse-phase HPLC chromatogram of purified Nr-13. The protein was loaded on a Vydac C 18 reverse-phase column, and detection was via UV absorbance at 214 nm. (C) Analytical size-exclusion chromatogram of Nr-13. The purified protein (41 μg/90 μL) was loaded on a Superose 12 column, and detection was via UV absorbance at 280 nm. The arrow denotes the void volume of the column (V_0). The first and second peaks were recovered within 3.5 and 5.2 min, corresponding to volumes of 1.4 and 2 mL, respectively. Bars mark the retention times for the standard proteins: a, bovine serum albumin (66 kDa); b, β-lactoglobulin (35 kDa); and c, cytochrome *c* (12.4 kDa).

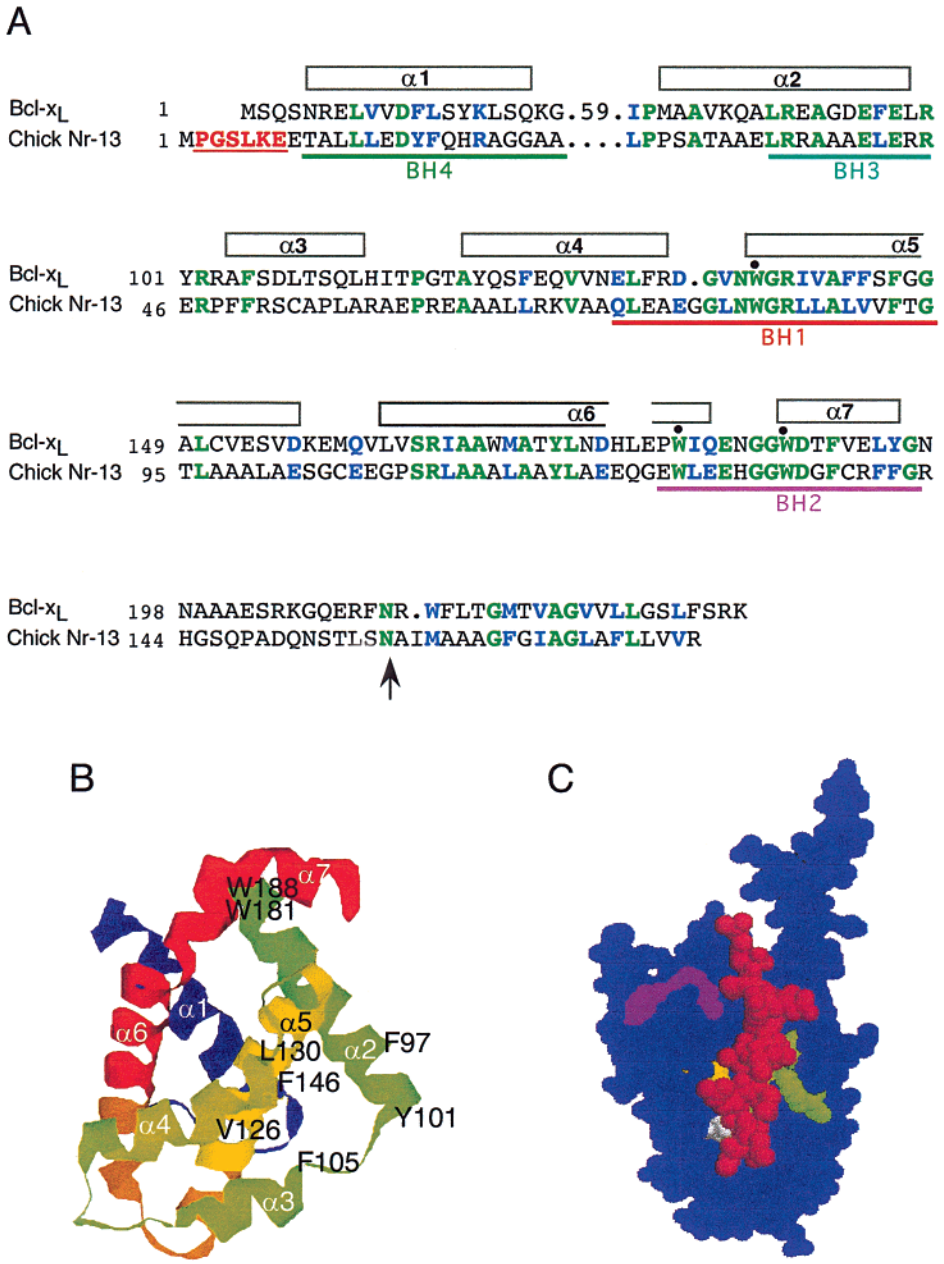

FIGURE 2: (A) Sequence alignment of chick Nr-13 (GenBank accession no. AF375661) and Bcl-x_L. Identical and similar residues are in green and blue, respectively. The BH1, BH2, BH3, and BH4 domains are shown in red, purple, blue, and green, respectively. The helices are denoted with boxes, based on the structure of Bcl-x_L (*7*). For the purpose of alignment, residues 22−80 of Bcl-x_L, corresponding to the long loop, are missing. The number 59 replaces these residues. The amino acid sequence of Nr-13 obtained by N-terminal sequencing of the protein is underlined and highlighted in red. Dots denote the conserved tryptophan residues. The arrow indicates the C-terminal end of the recombinant protein. (B) A ribbon representation of Bcl-xL. The coordinates of Bcl-xL were obtained from Protein Data Bank entry 1MAZ. The helices are distinguished by different colors. The key residues (F^{97}, F^{105}, V^{126}, L^{130}, and F^{146}) forming the hydrophobic cleft involved in BH3 binding are indicated, as well as conserved residues W^{137}, W^{181}, and W^{188}. (C) Surface representation of the Bcl-x_L−Bak-BH3 peptide. The coordinates of the complex were obtained from Protein Data Bank entry 1BXL. Bcl-x_L and the Bak peptide are shown in blue and red, respectively. Residues F^{97} and F^{146} are buried by the BH3 peptide, and the other hydrophobic residues are shown in green (F^{105}), yellow (L^{130}), or white (V^{126}). W^{137} and W^{181} are shown in magenta, and W^{188} cannot be seen in this view.

a tetramer as judged from its elution position. Assuming all the loaded protein is recovered in two elution peaks (Figure 1C), we can estimate concentrations of 8×10^{-8} M tetrameric Nr-13 and 9×10^{-7} M monomeric Nr-13 for the first and second peaks, respectively. The presence of Nr-13 in both peaks was ascertained by SDS−PAGE analysis (data not shown).

To estimate the level of folding of the purified protein, the secondary structure of recombinant Nr-13 was determined by CD spectroscopy. The CD spectrum of Nr-13 displayed intense negative bands at 208 and 222 nm which is characteristic for a prominent contribution of α-helices (Figure 4A). The helical content of the protein as calculated from the ellipticity at 222 nm (*27*) is ∼55−60%. The $[\theta]_{208}/[\theta]_{222}$ ratio of 1.1 is indicative of noninteracting α-helices (*34*). Fluorescence spectra were recorded to estimate the local environment of the tryptophan residues within the tertiary structure. The intrinsic fluorescence spectrum of purified Nr-13 showed that maximal emission was observed at 326 nm upon excitation at 295 nm (Figure 4B). For solution-exposed

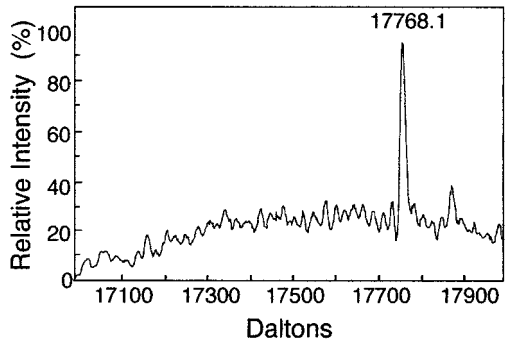

FIGURE 3: Deconvoluted electrospray mass spectrum of purified recombinant Nr-13. The eluted protein from the reverse-phase column (Figure 1B) was passed into the mass spectrometer. Mass spectra were acquired as indicated in Experimental Procedures.

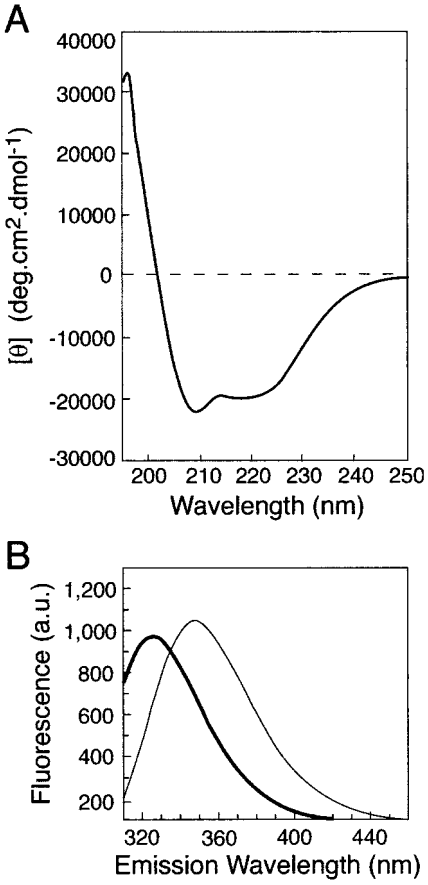

FIGURE 4: Circular dichroism and fluorescence spectra of Nr-13. (A) CD spectrum of purified Nr-13 in 20 mM Tris buffer (pH 8) containing 10 mM EDTA, 5% 2-propanol, and 0.5 mM DTT. The protein concentration was 40 μM. (B) The emission fluorescence of 0.4 μM Nr-13 (thick line) was recorded upon excitation at 295 nm in 1.2 mL of buffer at pH 8 (see Experimental Procedures) and corrected for buffer contribution. The fluorescence spectrum of 0.4 μM *N*-acetyltryptophanamide (thin line) was recorded under the same conditions and corrected for buffer contribution.

tryptophan, as mimicked by *N*-acetyltryptophanamide, maximal emission was found at 348 nm. This 22 nm blue shift indicates that the tryptophan residues of Nr-13 are localized within a hydrophobic environment.

Prevention of Caspase Activation by Nr-13. The biological activity of the purified protein was assessed in a cell-free system based on *Xenopus* egg extracts. This system presents spontaneous activation of caspases after a lag period of several hours (*35*). Consistently, Figure 5 shows that upon incubation at 25 °C, control *Xenopus* extracts exhibit caspase activation after a 3 h lag period. Addition of 20 μM Nr-13 at the beginning of the incubation prevented caspase activation, demonstrating the antiapoptotic activity of the purified protein. The same results were obtained with a lower concentration (3 μM) of Nr-13 (data not shown). In contrast, in the presence of BH3-Bax peptide, activation of caspase occurred within 1 h. Given that heterodimerization can modulate the activity of the apoptotic and antiapoptotic proteins, we tested whether Nr-13 could inhibit the caspase-activating effect of the BH3 domain of Bax. When stoichiometric amounts of Nr-13 and BH3-Bax peptide were incubated with *Xenopus* extracts, no caspase activation could be observed within 3 h of incubation, indicating that Nr-13 strongly counteracts the BH3 effect (Figure 5). As previously observed (*19*), the addition of exogenous cytochrome *c* to the extract results in an immediate activation of caspase-3.

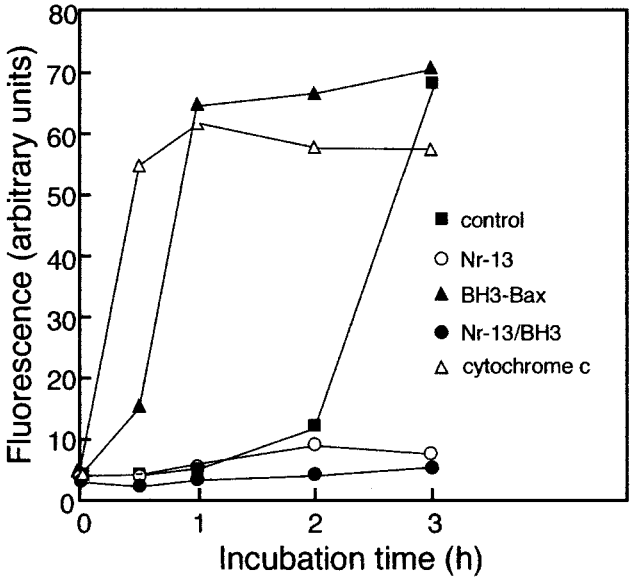

FIGURE 5: Inhibition of caspase activation in *Xenopus* egg extracts by Nr-13. *Xenopus* egg extracts were incubated in the presence of either purified Nr-13 in 20 mM Tris (pH 8) containing 10 mM EDTA, 5% 2-propanol, and 10 mM DTT (Nr-13); the buffer in which Nr-13 was stored (control); the peptide corresponding to the BH3 domain of Bax in the same buffer (BH3-Bax); both proteins at stoichiometric amounts (Nr-13/BH3); or cytochrome *c*. At the indicated times, samples were withdrawn and caspase activation was analyzed by cleavage of the fluorogenic substrate Ac-DEVD-AMC, as indicated in the Experimental Procedures. Caspase activation was detected by an increase in fluorescence emission at 460 nm upon excitation at 380 nm.

High-Affinity Binding of Nr-13 to Cytochrome c and BH3-Bax Peptide. Previous reports suggested an alternative pathway for preventing apoptosis by the antiapoptotic members of the Bcl-2 family; this implied a blockage of the release of cytochrome *c* from mitochondria (*18*, *19*). One can hypothesize that such a blockage might result from a direct interaction between the antiapoptotic proteins and cytochrome *c*. To check this hypothesis, the direct interaction between Nr-13 and cytochrome *c* was investigated by an ELISA in which cytochrome *c* or lysozyme, as an unrelated protein, was incubated with increasing amounts of Nr-13 (Figure 6A). Nr-13 specifically bound to immobilized cytochrome *c* since a saturation binding curve was obtained after correcting for a low level of unspecific interactions as

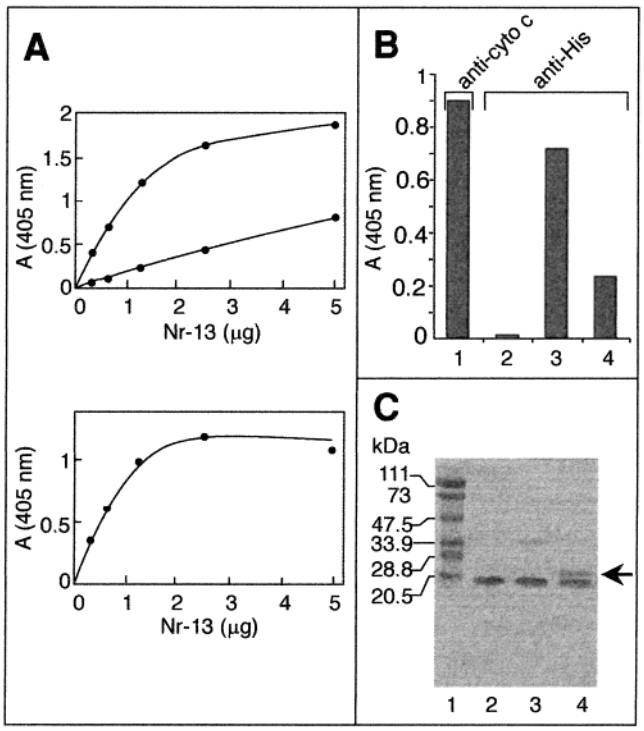

FIGURE 6: Binding of Nr-13 to cytochrome *c* and BH3-Bax. (A) In the top panel, 2.5 μg of either cytochrome *c* or lysozyme was adsorbed onto the plastic surface of an ELISA plate. After saturation of the nonspecific sites of the wells with 1% bovine serum albumin, increasing concentrations of Nr-13 in a total volume of 100 μL were added to the wells of microtitration plate. After a 1 h incubation at room temperature, the amount of Nr-13 bound to solid-phase cytochrome *c* (upper line) or lysozyme (lower line) was detected with an anti-His antibody followed by a peroxidase-conjugated second antibody, and addition of peroxidase substrate as described in Experimental Procedures. In the bottom panel, the difference between the level of binding to cytochrome *c* and the level of nonspecific binding to lysozyme, which bears positive charges similar to those of cytochrome *c*, is represented. (B) Cytochrome *c* (1 μg) adsorbed to the wells was detected by anti-cytochrome *c* antibody (lane 1, positive control) or anti-His antibody (lane 2, negative control). Solid-phase cytochrome *c* (1 μg) was incubated for 1 h with either 5 μg of Nr-13 (lane 3) or a mixture of 5 μg of Nr-13 and 9.3 μg (10-fold molar excess) of BH3-Bax peptide (lane 4) in a total volume of 100 μL. The amount of Nr-13 bound to the solid phase was detected with an anti-His antibody as described above. (C) Cross-linking of Nr-13 with BH3-Bax peptide. Nr-13 (15 μM) in the presence or absence of BH3-Bax was treated with glutaraldehyde (final concentration of 0.06%) for 20 min before analysis by SDS−PAGE and Coomassie Blue staining: lane 1, molecular mass markers; lane 2, Nr-13; lane 3, Nr-13 treated with glutaraldehyde; and lane 4, stoichiometric amounts of Nr-13 and BH3-Bax treated with glutaraldehyde. The arrow indicates the position of the cross-linked product.

estimated from the lysozyme data. The binding curve reached 50% saturation at an Nr-13 concentration of $\sim 4 \times 10^{-7}$ M. The accuracy of the ELISA technique was ascertained by the absence of interactions between the anti-His antibody and cytochrome *c* (Figure 6B, column 2), while the anti-cytochrome *c* antibody efficiently binds to cytochrome *c* (Figure 6B, column 1). The level of Nr-13 binding to cytochrome *c* was diminished by ~70% when Nr-13 was preincubated with BH3-Bax (Figure 6B, compare columns 3 and 4).

Binding of BH3-Bax to Nr-13 was monitored by cross-linking. Stoichiometric amounts of Nr-13 and BH3-Bax (15 μM each) incubated in the presence of glutaraldehyde formed a covalent complex which upon SDS−PAGE analysis migrates slower than Nr-13 (Figure 6C, lane 4). When Nr-13 was treated with glutaraldehyde in the absence of BH3-Bax, this band could not be observed (Figure 6C, lane 3). The difference of migration between the complex and Nr-13 corresponds to ca. 3 kDa which agrees well with the mass of 3300 Da of BH3-Bax as determined by mass spectrometry. This corroborates the above data in which similar concentrations of Nr-13 prevented the activation of caspases by BH3-Bax, indicating that the Nr-13−BH3-Bax interaction is biologically significant. Cross-linking experiments also indicated the presence of a dimeric form of Nr-13, since upon glutaraldehyde treatment a faint band appeared corresponding to a mass of 39 kDa (Figure 6C, compare lanes 2 and 3). Although less intense, this band was also visible in the presence of BH3-Bax. No band corresponding to a tetramer could be visualized after cross-linking. Similar results were obtained when ethylene glycol bis(succinimidyl succinate) was used as an alternative cross-linker at a final concentration of 0.9 mM (data not shown). Because of the presence of only two lysine residues within the Nr-13 sequence, the cross-linked products may not be the result of collisional cross-linking, even if this possibility cannot be completely ruled out. The use of a cross-linking experiment to assess binding of Nr-13 to cytochrome *c* was unsuccessful since cytochrome *c* alone, containing 19 lysine residues, was cross-linked into higher-molecular mass components (data not shown). This may be attributed to collisional cross-linking due to the high primary amino group content found in cytochrome *c*.

The interaction of Nr-13 with both cytochrome *c* and BH3-Bax was further characterized by quenching of the Nr-13 intrinsic tryptophan fluorescence. Incubation of 0.4 μM Nr-13 with increasing concentrations of cytochrome *c* led to a marked quenching of Nr-13 fluorescence, suggesting a direct binding to cytochrome *c* [Figure 7B (○)]. The Nr-13 spectral modifications showed a saturation dependence on cytochrome *c* concentration with a maximal quenching value of 27 ± 2%. This value reflects the average of quenching of the three tryptophans. The observed quenching was not due to fluorescence resonance energy transfer since the absorbance of reduced cytochrome *c*, which is very low between 300 and 380 nm, may hardly overlap with intrinsic fluorescence emission spectra of Nr-13 (Figure 4B, thick line). When Nr-13 was incubated under the conditions described above, with either the heme (0.2 and 0.8 μM) or insulin (0.4 μM) as a control (insulin does not contain any tryptophan residue), no change in quenching of Nr-13 was observed (data not shown). Moreover, when quenching was studied with a recombinant W127F mutant[2] under the same conditions that were used for wild-type Nr-13, no change was observed upon addition of cytochrome *c* within the concentration range used in Figure 7B. We verified by CD that this substitution does not modify the correct folding of the protein. In addition, this mutant exhibited lower antiapoptotic activity than wild-type Nr-13.[2] This indicates that the quenching observed for wild-type Nr-13 is not due to unspecific binding of Nr-13 with cytochrome *c*. Curve fitting using GraFit (*29*) resulted in an apparent dissociation constant of $(3.3 \pm 2.4) \times 10^{-8}$ M. Half-maximal quenching [Figure

[2] A. Barthelaix and M. Moradi-Améli, unpublished observations.

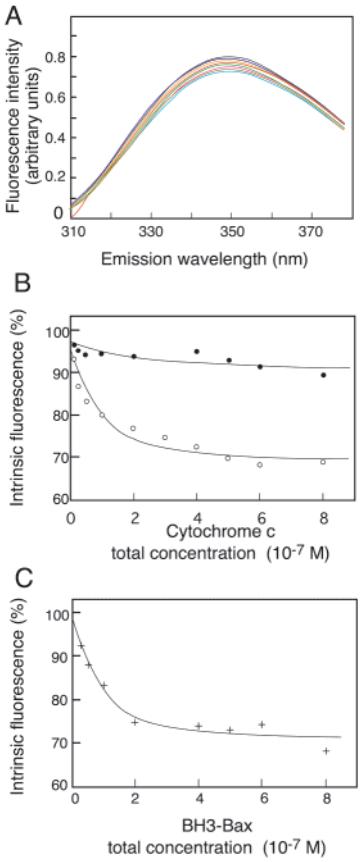

FIGURE 7: Nr-13 binding to cytochrome *c* and BH3-Bax as monitored by quenching of the intrinsic fluorescence. (A) Inner-filter effect of cytochrome *c*. The fluorescence spectrum of 0.4 μM NATA was recorded after excitation at 295 nm in 1.2 mL of buffer, at pH 8.0, in the absence of cytochrome *c* (upper black line) or in the presence of increasing concentrations (0.1, 0.2, 0.3, 0.4, 0.5, 0.6, and 0.8 μM from the purple line for the lowest concentration to the blue line for the highest concentration, respectively). Each trace was corrected by buffer subtraction. The slight decrease in NATA fluorescence following addition of cytochrome *c* is typical of the inner-filter effect which is due to the random absorbance of part of the exciting photons by cytochrome *c*. The highest cytochrome *c* concentration (0.8 μM) led to a slight decrease (up to 8%) in NATA fluorescence. (B) Interaction with cytochrome *c* as monitored by quenching of the intrinsic fluorescence of Nr-13. (○) The fluorescence spectra of 0.4 μM Nr-13 were recorded after excitation at 295 nm in the presence of increasing concentrations of cytochrome *c*. Each spectrum was corrected by buffer subtraction. The peak of intrinsic fluorescence emission was integrated between 310 and 380 nm and corrected for inner-filter effects of cytochrome *c* determined on NATA fluorescence as described for panel A. (●) Nr-13 (0.4 μM) was first preincubated for 15 min in the presence of 0.2 μM BH3-Bax, and then the fluorescence spectra of Nr-13 were recorded after excitation at 295 nm in the presence of increasing concentrations of cytochrome *c* as described above. Maximal and minimal quenching values as well as dissociation constants were determined using GraFit (*29*), taking into account a final concentration of 0.1 μM for Nr-13. The traces are computed curves generated with the GraFit software. They are characterized by the following parameters: (○) $F_{max} = 95.4 \pm 1.8$ and $F_{min} = 68.6 \pm 2.3$ and (●) $F_{max} = 97.2 \pm 1.2$ and $F_{min} = 89.6 \pm 3.3$. (C) Interaction with BH3-Bax as monitored by the quenching of intrinsic fluorescence. The fluorescence spectra of 0.4 μM Nr-13 were recorded after excitation at 295 nm in the presence of increasing concentrations of BH3-Bax. Each spectrum was corrected by buffer subtraction. The peak of intrinsic fluorescence emission was integrated between 310 and 380 nm and corrected for inner-filter effects of BH3-Bax. The computed curves present the following parameters: $F_{max} = 98.8 \pm 1.6$ and $F_{min} = 70.3 \pm 1.7$. In panels B and C, the total ligand concentration is indicated on the abscissa.

7B (○)] is observed at $\sim 8 \times 10^{-8}$ M added cytochrome *c*. The 4−5-fold higher value observed in ELISA experiments might reflect changes due to binding of the protein to the surface of the ELISA plate and/or to the fact that this technique does not allow experimentation under equilibrium binding conditions. A low concentration of ligand (10^{-7} M) can induce significant quenching of Nr-13 tryptophan [Figure 7B (○)]. However, such a quenching should occur at a lower Nr-13/ligand molar ratio and is not consistent with the high Nr-13 concentration of 4×10^{-7} M used in this assay (as measured by the Bradford assay for monomeric Nr-13 and estimated by Coomassie Blue staining of Nr-13 following SDS−PAGE). This discrepancy is also observed when using GraFit (*29*). The program required an Nr-13 concentration of 0.1 μM instead of 0.4 μM for calculation of K_D. Such a discrepancy between the experimental and theoretical concentration of Nr-13 might be explained assuming that the interacting form of Nr-13 is a tetramer. The presence of tetrameric Nr-13 as found by gel permeation (see Figure 1C) supports this suggestion.

A marked quenching of Nr-13 intrinsic fluorescence was also observed upon incubation with increasing concentrations of BH3-Bax with a maximal value of 28 ± 2% (Figure 7C). An apparent dissociation constant of $(2.8 \pm 1.5) \times 10^{-8}$ M could be determined using a curve fitting program assuming an Nr-13 concentration of 0.1 μM instead of 0.4 μM, suggesting that the tetramer appears to be the interacting form. Half-maximal quenching was achieved at 6×10^{-8} M BH3-Bax (Figure 7C). When Nr-13 reached maximal quenching after preincubation for 15 min with BH3-Bax, no further reduction in fluorescence could be observed by subsequent addition of increasing concentrations of cytochrome *c* [Figure 7B (●)]. Only a low level of residual quenching was observed, reaching 8% for high concentrations of cytochrome *c*. This leads to the following suggestions. (i) A conformational change of Nr-13 may occur upon binding of Nr-13 to BH3-Bax which alters its ability to bind cytochrome *c*. (ii) Given that both ligands, exhibiting similar K_D values, produced similar fluorescence quenching, an exchange between ligands may occur which would not induce any additional change in fluorescence. This residual quenching agrees with the prevention of Nr-13 binding to immobilized cytochrome *c* in an ELISA (see Figure 6B). An apparent discrepancy exists between the 8% level of residual quenching and the 30% level of residual binding of Nr-13 to immobilized cytochrome *c* in ELISA experiments. This higher level of residual binding may be explained by a low level of unspecific interaction between Nr-13 and the immobilized protein (as observed in Figure 6A), and/or an exchange between ligands (cytochrome *c* and BH3-Bax) for binding to Nr-13 that may occur during the 1 h incubation in the latter experiments.

DISCUSSION

The aim of this work was to purify the antiapoptotic protein Nr-13 to homogeneity in its biologically active form to characterize the binding properties of this protein of the Bcl-2 family. Nr-13 was prepared and purified by (i) removal of the putative C-terminal transmembrane domain to enhance the solubility, (ii) fusion with a C-terminal hexahistidine tag, and (iii) use of a special *E. coli* host strain to prevent the problem of toxicity of the expression plasmid. The standard

purification protocol consisting of affinity chromatography followed by anion exchange chromatography proved to be insufficient which is probably due to the rather poor solubility of Nr-13 and its tendency to aggregate with other proteins. A second anion exchange chromatography step allowed the preparation of the highly pure protein as ascertained by the presence of a single peak upon reverse-phase chromatography. Elution of the purified protein on the reverse-phase column required an acetonitrile concentration of as high as 60%, indicating that the whole molecule was hydrophobic. Both amino-terminal sequencing and mass spectrometry confirmed the identity of the purified protein as Nr-13 and showed that the initiating methionine was removed. Our data support the idea that Nr-13 is structurally related to Bcl-x_L, and that recombinant Nr-13 adopts a nativelike conformation. Consistent with the structure of Bcl-x_L which is 60% α-helical (*7*, *10*), CD studies indicate that Nr-13 has a 55−60% α-helical conformation. W^{137} and W^{181} of Bcl-x_L, which are equivalent to W^{83} and W^{127} of Nr-13, respectively (see Figure 2), have been reported to be located in the vicinity of a hydrophobic BH groove with their side chains exposed in the central area of the groove (*7*, *33*). Consistently, tryptophans 83 and 127 of the BH1 and BH2 domains, respectively, seem to be located within a hydrophobic environment as evidenced by the low wavelength for maximal fluorescence emission, 326 nm, which is markedly blue shifted (22 nm) when compared to that of solution-exposed *N*-acetyltryptophanamide.

Critical functions of Bcl-2-like proteins are thought to be modulated by the formation of dimers (*36*, *37*). The proapoptotic protein Bax was reported to form large oligomers, while antiapoptotic proteins such as Bcl-2 and Bcl-x_L were essentially monomeric (*38*, *39*). A fraction of the Nr-13 population (20%) running through a gel permeation column is found to be under a tetrameric state. When the pressure applied to the protein during chromatography which tends to dissociate multimers is considered, it is likely that tetrameric Nr-13 represents more than 20% of the total Nr-13 population. The presence of dimeric Nr-13 instead of the tetramer in cross-linking experiments may be explained assuming that due to steric constraints the tetramer in solution is formed by two asymmetric dimers. The use of a diluted protein solution and short times of incubation (*40*), as well as the presence of a few reactive primary amino groups in Nr-13 (2 K), reduce the possibility of collisional interactions.

The ability of Nr-13 to prevent caspase activation in a cell-free system provides strong evidence that the molecule is functionally active. Nr-13 might exert its antiapoptotic activity at the mitochondrial level since in *Xenopus* egg extracts system caspase activation was reported to be due to a spontaneous release of cytochrome *c* from mitochondria (*19*, *41*). In agreement with our data, the BH3 domain from proapoptotic Bcl-2 proteins was reported to trigger apoptosis in *Xenopus* egg extracts, likely by binding endogenous proteins of the Bcl-2 family that may be present in the extracts (*31*). Our experiments of titrating the activity of BH3-Bax peptide against exogenous Nr-13 show that the interaction of a BH3 domain with Nr-13 neutralizes the ability of BH3 to trigger apoptosis. Interestingly, this interaction does not turn Nr-13 into a proapoptotic molecule; on the contrary, it completely abrogates the ability of BH3 to induce apoptosis. This suggests that the antiapoptotic function of Nr-13 may dominate the proapoptotic function of BH3-Bax and is consistent with the recently reported capacity of Nr-13 to antagonize the death-inducing effect of Bax in yeast (*42*).

Studies using recombinant proteins suggest that both homo- and heterodimers can be disrupted by interaction with peptides derived from BH3 domains of Bax or Bak with an apparent micromolar affinity (*43*). In accordance with previous data on the binding of Nr-13 to Bax (*23*), an interaction between BH3-Bax and Nr-13 is reported from cross-linking experiments. This can be correlated with the above results on the function of Nr-13 in neutralizing the BH3-Bax effect. The affinity of this interaction was measured by quenching of the fluorescence emission of Nr-13 tryptophan residues. A low apparent dissociation constant of 28 nM was determined, compared to the dissociation constants reported for the interaction of either Bcl-x_L with Bak- and Bax-BH3 (0.2 and 13 μM, respectivel; *10*), or Bcl-2 with Bax-BH3 (0.14 μM; *44*) and to the above-mentioned affinities (*43*). While tetrameric Nr-13 seems to be the interacting form trapping the BH3 peptide, it is likely that this oligomeric state dissociates further into a heterodimer containing monomeric Nr-13 since only the latter form is cross-linked with the peptide. This is as well supported by the 1/1 stoichiometry observed in other complexes formed by antiapoptotic proteins and BH3 peptides (*10*, *43*) and by the model proposed below for the Nr-13−BH3 complex. Binding data may alternatively be explained assuming that a substoichiometric amount of monomeric ligand induces a change in the Nr-13 conformation, resulting in a change in fluorescence. The structure of the Bcl-x_L−BH3-Bak complex revealed that the insertion of the BH3 domain into the hydrophobic cleft of Bcl-x_L is a key event in the heterodimerization process (*10*) (see Figure 2C). The complex is essentially stabilized by four highly conserved hydrophobic side chains of the Bak helix (V^{74}, L^{78}, I^{81}, and I^{85}) pointing to the hydrophobic cleft of Bcl-x_L (*10*). By analogy, and because of the sequence similarity between BH3-Bak and -Bax and the known structure of Bax (*9*), a model can be proposed in which residues L^{59}, L^{63}, I^{65}, and L^{70} of Bax-BH3 may direct their side chains to the hydrophobic cleft of Nr-13. According to this model, the high-affinity hydrophobic interaction thus induces tight heterodimerization, producing complete disruption of the multimeric state of Nr-13. Residue Y^{101} has been reported to be crucial for the interaction of Bcl-x_L with BH3 (*10*), and a Y101K substitution abolished this interaction (*45*). In Nr-13, however, the residue corresponding to Y^{101} is E^{46} (Figure 2A); nonetheless, this seems not to interfere with its functional activity or its binding to the BH3 domain of Bax. Nr-13, as another antiapoptotic protein, is located at the outer mitochondrial membrane,[3] while Bax is translocated from the cytosol to this membrane after induction of apoptosis (*46*). On the basis of this localization, our data suggest that in the physiological context, one of the functions of Nr-13 is to neutralize the Bax apoptotic activity via a BH3-dependent mechanism at the mitochondrial level.

Blockage of cytochrome *c* release from mitochondria by the antiapoptotic members of the Bcl-2 family has been reported as an alternative pathway for the prevention of

[3] A. Aouacheria and G. Gillet, unpublished observations.

apoptosis (*18*, *19*). However, the mechanism by which Bcl-2 proteins are able to block the release remains unknown. In the study presented here, our data support a direct interaction between Nr-13 and cytochrome *c*. In fact, the binding of either immobilized or soluble cytochrome *c* to the well-folded and active recombinant protein Nr-13 occurs with high specificity and high affinity. An apparent dissociation constant of 33 nM was obtained for tetrameric Nr-13. Interestingly, the presence of the tetrameric form at such a low concentration was also shown by gel permeation experiments. This K_D value is within the same range as that of Nr-13 in complex with the BH3 peptide, which produced a similar maximal quenching of the intrinsic fluorescence. Theses changes in Nr-13 fluorescence were correlated to the level of specific binding of either cytochrome *c* or BH3-Bax since no effect at all was observed in control experiments with either the heme alone or an unrelated protein. By analogy with BH3-Bax interaction, a disruption of tetrameric Nr-13 into its monomeric form following cytochrome *c* binding cannot be excluded. Once released from mitochondria, the cytochrome *c* binds strongly to Apaf-1, with an association constant of 4×10^7 M^{-1} (*47*). The association constant of the Nr-13−cytochrome *c* interaction (3×10^7 M^{-1}) was similar to that of the Apaf-1−cytochrome *c* interaction. Such similarity showed that the affinity of binding of Nr-13 to cytochrome *c* might be of biological relevance. Due to the large positively charged surface of cytochrome *c*, its putative binding site on Nr-13 may rather correspond to a negatively charged area. For being able to interact with cytochrome *c*, such a binding site on Nr-13 should be able to face the inner membrane space (IMS) of the mitochondria. In fact, Nr-13 possesses, like other Bcl-2-like proteins (*7*−*9*), two central helices (α-helices 5 and 6) which are thought to cross the outer mitochondrial membrane.

The interaction between Nr-13 and cytochrome *c* is prevented by heterodimerization of Nr-13 with the proapoptotic BH3 domain. However, it is unlikely that both cytochrome *c* and BH3 peptide share the same binding site on Nr-13, since the hydrophobic cleft forming the binding site for BH3 (see above) is not consistent with the ionic strength dependence of cytochrome *c* binding. Therefore, the antagonism between the two ligands may likely be due to a conformational change induced by the binding of the BH3 peptide, which in turn buries the binding site for cytochrome *c*. In support of this hypothesis, a conformational change of Bcl-x_L upon addition of Bak-BH3 peptide has been observed in an NMR study (*10*).

Taken together, our data demonstrate a direct interaction between an antiapoptotic protein and cytochrome *c*, whereas an association between Bcl-x_L and cytochrome *c* was also observed by Kharbanda et al. (*48*) using co-immunoprecipitation. How the interaction between Nr-13 and cytochrome *c* could occur in the physiological context is an open question. However, our results suggest that Nr-13 may regulate cell survival, at the mitochondrial level, by two distinct mechanisms. First, Nr-13 by interacting with the BH3 domain of Bax may prevent opening of the VDAC and the release of cytochrome *c* in the cytosol through this channel, as already proposed for Bcl-x_L (*20*). Second, Nr-13 may directly bind to cytochrome *c*, preventing its release and subsequent caspase activation.

ACKNOWLEDGMENT

We are grateful to Dr. J. E. Walker (Medical Research Council, Cambridge, U.K.) for the kind gift of *E. coli* strain C41(DE3). We thank Dr. J. C. Cortay for providing vector pT7-7 encoding the six-His codon, Dr. Konrad Beck for critical reading of the manuscript and numerous suggestions, Dr. E. Auber-Foucher for helpful discussions, R. Montserret for CD measurements, M. Corteau for N-terminal sequencing, and C. van Herrewege for the artwork.

REFERENCES

1. Reed, J. C. (1997) *Nature 387*, 773−776.
2. Adams, J. M., and Cory, S. (1998) *Science 281*, 1322−1326.
3. Chao, D. T., and Korsmeyer, S. J. (1998) *Annu. Rev. Immunol. 16*, 395−419.
4. Thompson, C. B. (1995) *Science 267*, 1456−1462.
5. Gross, A., McDonnell, J. M., and Korsmeyer, S. J. (1999) *Genes Dev. 13*, 1899−1911.
6. Hengartner, M. O. (2000) *Nature 407*, 770−776.
7. Muchmore, S. W., Slatter, M., Liang, H., Meadows, R. P., Harlan, J. E., Yoon, H. S., Nettesheim, D., Chang, B. S., Thompson, C. B., Wong, S. L., Ng, S. C., and Fesik, S. W. (1996) *Nature 381*, 335−341.
8. Chou, J. J., Li, H., Salvesen, G. S., Yuan, J., and Wagner, G. (1999) *Cell 96*, 615−624.
9. Suzuki, M., Youle, R. J., and Tjandra, N. (2000) *Cell 103*, 345−354.
10. Sattler, M., Liang, H., Nettesheim, D., Meadows, R. P., Harlan, J. E., Eberstadt, M., Yoon, H. S., Shuker, S. B., Chang, B. S., Minn, A. J., Thompson, C. B., and Fesik, S. W. (1997) *Science 275*, 983−986.
11. Minn, A. J., Velez, P., Schendel, S. L., Liang, H., Muchmore, S. W., Fesik, S. W., Fill, M., and Thompson, C. B. (1997) *Nature 385*, 353−357.
12. Schlesinger, P. H., Gross, A., Yin, X. M., Yamamoto, K., Saito, M., Waksman, G., and Korsmeyer, S. J. (1997) *Proc. Natl. Acad. Sci. U.S.A. 94*, 11357−11362.
13. Shimizu, S., Ide, T., Yanagida, T., and Tsujimoto, Y. (2000) *J. Biol. Chem. 275*, 12321−12325.
14. Ahsen, O. V., Waterhouse, N. J., Kuwana, N. J., Newmeyer, D. D., and Green, D. R. (2000) *Cell Death Differ. 12*, 1192−1199.
15. Narita, M., Shimizu, S., Ito, T., Chittenden, T., Lutz, R. J., Matsuda, H., and Tsujimoto, Y. (1998) *Proc. Natl. Acad. Sci. U.S.A. 95*, 14681−14686.
16. Shimizu, S., Eguchi, Y., Kamiike, W., Funahashi, Y., Mignon, A., Lacronique, V., Matsuda, H., and Tsujimoto, Y. (1998) *Proc. Natl. Acad. Sci. U.S.A. 95*, 1455−1459.
17. Vander Heiden, M. G., Chandel, N. S., Schumaker, P. T., and Thompson, C. B. (1999) *Mol. Cell 3*, 159−167.
18. Yang, J., Liu, X., Bhalla, K., Kim, C. N., Ibrado, A. M., Cai, J., Peng, T., Jones, D. P., and Wang, X. (1997) *Science 275*, 1129−1132.
19. Kluck, R. M., Bossy-Wetzel, E., Green, D. R., and Newmeyer, D. D. (1997) *Science 275*, 1132−1136.
20. Shimizu, S., Narita, M., and Tsujimoto, Y. (1999) *Nature 399*, 483−487.
21. Gillet, G., Guerin, M., Trembleau, A., and Brun, G. (1995) *EMBO J. 14*, 1372−1381.
22. Mangeney, M., Schmitt, J. R., Leverrier, Y., Thomas, J., Marvel, J., Brun, G., and Gillet, G. (1996) *Oncogene 13*, 1441−1446.
23. Lee, R. M., Gillet, G., Burnside, J., Thomas, S. J., and Neiman, P. (1999) *Genes Dev. 13*, 718−728.
24. Miroux, B., and Walker, J. E. (1996) *J. Mol. Biol. 260*, 289−298.
25. Bradford, M. M. (1976) *Anal. Biochem. 72*, 248−251.
26. Rousseau, J. C., Farjanel, J., Boutillon, M. M., Hartman, M., van der Rest, M., and Moradi-Améli, M. (1996) *J. Biol. Chem. 271*, 23743−23748.
27. Chen, Y. H., and Yang, J. T. (1971) *Biochem. Biophys. Res. Commun. 44*, 1285−1291.
28. Merrifield, R. B. (1964) *Biochemistry 3*, 1385−1390.
29. Divita, G., Goody, R. S., Gautheron, D. C., and Di Pietro, A. (1993) *J. Biol. Chem. 268*, 13178−13186.
30. Kornbluth, S. (1997) *Methods Enzymol. 283*, 600−614.
31. Cosulich, S. C., Worrall, V., Hedge, P. J., Green, S., and Clarke, P. R. (1997) *Curr. Biol. 7*, 913−920.

32. Lazebnik, S. H., Kaufmann, S. H., Desnoyers, S., Poirier, G. G., and Earnshaw, W. C. (1994*) Nature 371*, 346−347.
33. Aritomi, M., Kunishima, N., Inohara, N., Ishibashi, Y., Ohta, S., and Morikawa, K. (1997) *J. Biol. Chem. 272*, 27886−27892.
34. Monera, O. D., Kay, C. M., and Hodges, R. S. (1994) *Protein Sci. 3*, 1984−1991.
35. Cosulich, S. C., Green, S., and Clarke, P. R. (1996) *Curr. Biol. 6*, 997−1005.
36. Oltvai, Z. N., and Korsmeyer, S. J. (1994) *Cell 79*, 189−192.
37. Yang, E., Zha, J., Jockel, J., Boise, L. H., Thompson, C. B., and Korsemeyer, S. J. (1995) *Cell 80*, 285−291.
38. Antonsson, B., Montessuit, S., Lauper, S., Eskes, R., and Martinou, J.-C. (2000) *Biochem. J. 345*, 271−278.
39. Conus, S., Kaufmann, T., Fellay, I., Otter, I., Rosse, T., and Borner, C. (2000) *EMBO J. 19*, 1534−1544.
40. Middaugh, C. R., Vanin, E. F., and Ji, Th. (1983) *Mol. Cell. Biochem. 50*, 115−141.
41. Kluck, R. M., Esposti, M. D., Perkins, G., Renden, C., Kuwana, T., Bossy-Wetzel, E., Goldberg, M., Allen, T., Barber, M. J., Green, D. R., and Newmeyer, D. D. (1999) *J. Cell Biol. 147*, 8209−8212.
42. Aouacheria, A., Arnaud, E., Venet, S., Lalle, P., Gouy, M., Rigal, D., and Gillet, G. (2001) *Oncogene 20*, 5846−5855.
43. Diaz, J. L., Oltersdorf, T., Home, W., McConnell, M., Wilson, G., Weeks, S., Garcia, T., and Fritz, C. (1997) *J. Biol. Chem. 272*, 11350−11355.
44. Anderson, M., Blowers, D., Hewitt, N., Hedge, P., Breeze, A., Hampton, I., and Taylor, I. (1999) *Protein Expression Purif. 15*, 162−170.
45. Minn, A. J., Kettlun, C. S., Liang, H., Kelatar, A., Vander Heiden, M. G., Chang, B. S., Fesik, S. W., Fill, M., and Thompson, C. B. (1999) *EMBO J. 18*, 632−643.
46. Hsu, Y. T., Wolter, K. G., and Youle, R. J. (1997) *Proc. Natl. Acad. Sci. U.S.A. 94*, 3668−3672.
47. Purring-Koch, C., and McLendon, G. (2000) *Proc. Natl. Acad. Sci. U.S.A. 97*, 11928−11931.
48. Kharbanda, S., Pandey, P., Schofield, L., Israels, S., Roncinske, R., Yoshida, K., Bharti, A., Yuan, Z. M., Saxena, S., Weichselbaum, R., Nalin, C., and Kufe, D. (1997) *Proc. Natl. Acad. Sci. U.S.A. 94*, 6939−6941.

BI0110286